



Instabilities of nematic liquid crystal films

L. Kondic^a and L. J. Cummings^a

Abstract

We discuss instabilities exhibited by free surface nematic liquid crystal (NLC) films of nanoscale thickness deposited on solid substrates, with a focus on surface instabilities that lead to dewetting. Such instabilities have been discussed extensively; however, there is still no consensus regarding the interpretation of experimental results, appropriate modeling approaches, or instability mechanisms. Instabilities of thin NLC free surface films are related to a wider class of problems involving dewetting of non-Newtonian fluids. For nanoscale films, the substrate–film interaction, often modeled by a suitable disjoining pressure, becomes relevant. For NLCs, one can extend the formulation to include the elastic energy of the NLC film, leading to an ‘effective’ disjoining pressure, playing an important role in instability development. Focusing on thin film modeling within the framework of the long-wave asymptotic model, we discuss various instability mechanisms and outline problems where new research is needed.

Addresses

Department of Mathematical Sciences, New Jersey Institute of Technology, Newark, NJ, 07102, USA

Corresponding author: Kondic, L. (kondic@njit.edu)

^a <https://cfsm.njit.edu>

Current Opinion in Colloid & Interface Science 2021, 55:101478

This review comes from a themed issue on **Wetting and Spreading**

Edited by **Tatiana Gambaryan-Roisman** and **Victor Starov**

For a complete overview see the [Issue](#) and the [Editorial](#)

<https://doi.org/10.1016/j.cocis.2021.101478>

1359-0294/© 2021 Elsevier Ltd. All rights reserved.

Keywords

Thin fluid films, Nematic liquid crystals, Fluid instabilities, Free surface flow.

Introduction

With the increasing use of liquid crystal–based displays (LCDs), driven by the evolution of portable electronic devices, the desire to minimize paper waste, and the popularity of flat panel displays, liquid crystals (LCs), in particular nematic LCs (NLCs), remain important industrial materials. Although they are well studied, novel and evolving applications continue to open new research directions. For example, LCDs fabricated from polymers

(rather than the traditional glass bounding surfaces) are opening the doors to a new generation of flexible LCD devices that are lightweight, easily stowed, and nearly unbreakable [51]. Other existing and emerging applications of nematic (and other) LCs abound: LCs are finding new applications in photovoltaics, biosensors, plasmonics, opto-fluidics, and more; see the review article by Palffy-Muhoray [55] for an overview. On the theoretical side, the comprehensive review by Rey and Denn [64] discusses various aspects involved in the modeling of LC dynamics and provides much useful background.

In addition to numerous direct applications, NLCs are becoming increasingly relevant as a model system for more complex active matter systems, which often involve (active) particles with a nematic or similar type of structure. Such connections between LC films and various fields of research in the wider soft matter and fluid dynamic communities have been recently discussed in a number of excellent reviews. A review by Marchetti et al. [50] focuses on active matter, but also considers a number of issues relevant to LCs. Saintillan [65**] provided an overview of computational models relevant to active fluids and LCs, whereas the state of the art in more general computational modeling of LCs was reviewed in 2019 by Allen [1]. Rey [63] surveys the application of LC models in various biological settings, whereas Sengupta [68] reviews the recent interest in exploiting the unique optical properties of LCs within the context of topological microfluidics, and Jákli et al. [31*] discuss novel aspects of LCs comprising banana-shaped molecules. Interaction of LCs with external fields, vital for many applications, has been reviewed extensively as well—for example, the well-studied interaction of NLCs with external light sources was reviewed by Demeter and Krimer [16] and the spreading of dielectric films (including NLCs) under electric field gradients in a dielectrowetting setup, by Edwards et al. [19*].

LC films may be subject to instabilities of various types and origins. Examples include instabilities of the director field in confined layers due to external forcing, as reviewed and studied recently by Gartland [23], as well as instabilities of flowing [27,36] or deposited [56,15] free surface films, as considered in this review. Free surface films on the nanoscale, when deposited on solid substrates, are themselves subject to different types of

Supported by NSF Grants no. DMS-1815613 and CBET-1604351.

destabilizing mechanisms: dewetting, resulting either from destabilizing film–substrate interactions (spinodal dewetting) [66] or the presence of defects (nucleation) [30], as well as ‘fingering’ type instabilities relevant to setups involving propagating fronts [36]. In this brief review, we focus only on the former case: dewetting of free-surface NLC films of nanoscale thickness, deposited on substrates. In addition to the motivation discussed previously, these instabilities are of interest because they allow, at least in principle, for a more detailed understanding of the connection between the instabilities and the approaches used to model NLC rheology, as well as the interaction of NLCs with the underlying substrates. Correlation of model outcomes with the experimental results could lead to the development of more realistic models. We discuss in particular the (common) setup of antagonistic anchoring, where the rod-like NLC molecules have different preferred directions at the interface between the NLC film and the substrate and at the NLC film (free) surface. Such setups have been studied for at least three decades now (see, e.g. the review by Jerome [32]), but are still not completely understood. Antagonistic anchoring (if strong) leads to an additional singularity at a contact line where the three phases (NLC, solid, and air) meet because of the large elastic energy cost for the NLC molecules to accommodate the antagonistic anchoring conditions. Such a singularity is distinct from the well-known contact line singularity that is present even for Newtonian fluids in setups involving static and dynamic contact lines; see the reviews by Craster and Matar [10] and Bonn et al. [7] for further discussion.

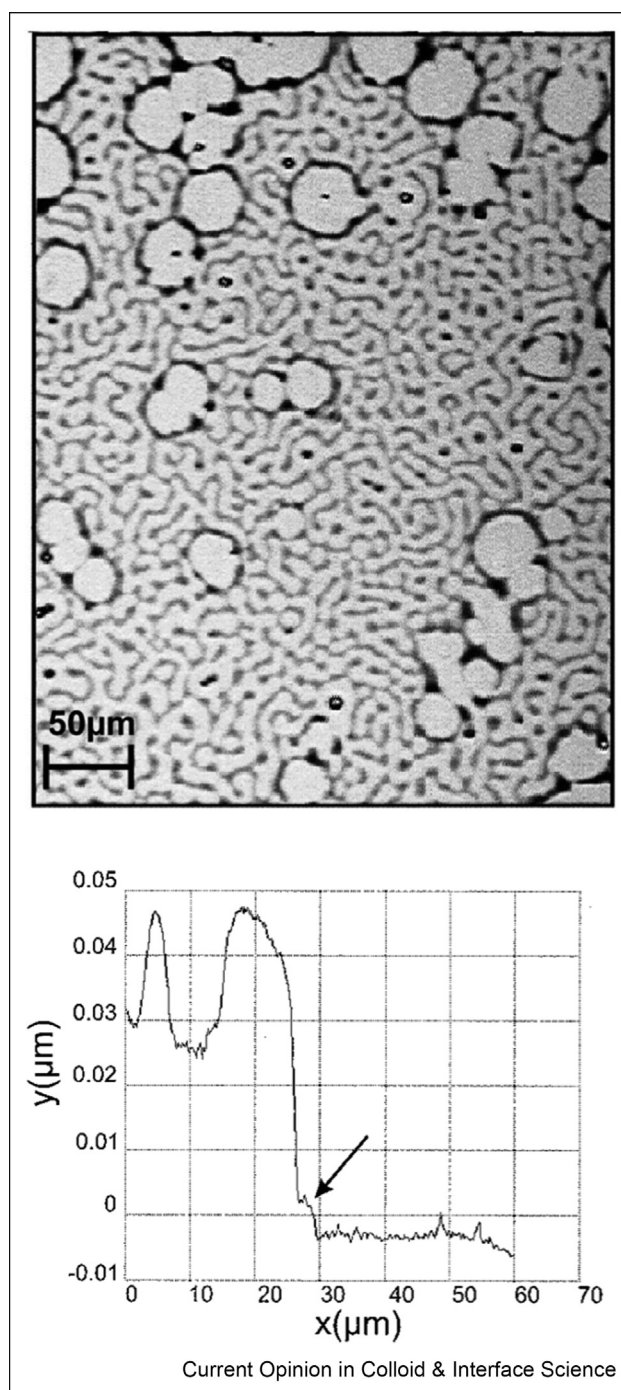
The remaining part of this article is organized as follows. In Section [Background](#), we provide a general review of free surface instabilities in deposited thin films of NLCs. Section [Modeling of free surface NLC films](#) then gives a brief overview of the modeling techniques, with a focus on the Leslie-Ericksen LC description. Section [Instabilities](#) is devoted to a discussion of selected recent results in the field. We conclude with a summary in Section [Conclusion](#).

Background

Over the last two-plus decades, a body of experimental work on thin NLC free surface films has been assembled, and its significance was discussed by various groups (see e.g. Refs. [14,15,20,21,30,57,58,66,77,79]). Collectively, this work demonstrates that NLC films can exhibit extremely complex spreading and dewetting phenomena and builds a detailed and intriguing picture of how they behave under a range of conditions. However, the studies, outlined next, raise as many questions as they answer, and there is no consensus on how to interpret the data, particularly when films of thickness of tens or hundreds of nm are concerned [15,21,75,79,80].

[Figure 1](#) (from Ref. [30]) shows a thin film of the NLC 5AB₄ coating a silicon wafer. [Figure 1A](#) is a micrograph in which the grayscale indicates the film height (lighter regions are thinner). Starting from an initially flat film, circular dewetted patches appear almost immediately, followed by undulations. [Figure 1B](#) shows the height profile of a subset of 1A (at the edge of a dewetted

Figure 1



Dewetting patterns in a thin film (average thickness 40 nm) of 5AB₄ on silicon [30].

patch) generated via scanning force microscopy. Figures 1A and B together clearly show the existence of distinct lateral and vertical length scales, suggesting that the instability may be described by a long-wave analysis because the in-plane dimensions (measured in microns) are much larger than the out-of-the plane one (measured in tens of nanometers). These length scales as well as the typical time scale of the instability development (measured in seconds to minutes) provide some input to the modeling efforts.

Following this early work, van Effenterre et al. [20] considered the behavior of nanoscale thickness films of the NLC 5CB on silicon as temperature was varied. It was found that above the transition temperature (the isotropic state), the film remained flat, whereas below transition, the film developed patterns of thickness variation on a distinct length scale. The authors attributed the thickness variations to a coexistence of phases, thinner regions being isotropic and thicker ones nematic, although patterns are only observed below the nematic transition temperature. Two years later, a subset of the same group published a simple steady-state energetics model [21]: assuming that elastic distortions are sustained in the thicker nematic regions, the authors claimed that coexistence could be explained. Another contemporaneous study by Zihler and Zumer [79], however, argued that the isotropic state could not coexist with the nematic in the temperature range studied; the evidence presented in the study by van Effenterre et al. [20] supporting the isotropic regions was in fact consistent with a nematic state, and moreover, the elastically distorted director configuration needed for the theory of van Effenterre et al. [20] was energetically far too costly. Instead, it was proposed a ‘pseudo Casimir’ effect, based on director fluctuations within the thin film, could explain the observations. This discussion was continued without resolution in follow-up works [74,80]. To add to the debate, additional experiments with NLCs 5CB and 8CB were carried out by Schlagowski et al. [66] meanwhile, the results of which were used to suggest that the instability mechanism is related to textures (caused by defects) of NLCs and that neither elastically distorted director configurations nor pseudo-Casimir effects are relevant. The problem was revisited a few years later by Delabre et al. [15], who declared that neither the isotropic-nematic coexistence model [75] nor the pseudo-Casimir model [79] convincingly fitted the observations, but that, within the thicker film regions at least, significant director elastic distortion exists. The authors conclude: “a proper description of ... films thinner than 50 nm is required. ... The most difficult task is to write properly the short-range structural contribution ... crucial for a quantitative description of the observed thickness coexistence” and “an elastic term must be included in the disjoining pressure” [15].

The approach based on steady-state energetics, discussed previously, provides an important input to studies focusing on the dynamics of nanoscale NLC films, in particular regarding the nature of the NLC film—solid substrate interaction, discussed in more detail later in the review. Regarding dynamical considerations per se, the relevant research has been so far rather limited. One approach to this task is to carry out molecular dynamic simulations; this was the approach implemented by Nguyen et al. [53], with interactions simulated via Gay-Berne [24] and modified Lennard-Jones 6–12 potentials. The results show good qualitative agreement with experimental data, but with 10^7 particles simulated (representing a system of only very modest size), the computational run time is still significant even on supercomputers. The results are also consistent with those obtained using asymptotically simplified models, which are much faster to simulate numerically and are, to some extent, amenable to analytical approaches. This approach is discussed next.

Modeling of free surface NLC films

We focus our modeling description on the simplest Leslie-Ericksen approach [22,42], as also considered by other authors [49,48,61,8], and refer the reader to other sources (such as Rey and Denn [64]) for a review of the complementary Landau-de Gennes [12] theory. Starting from the full Leslie-Ericksen model equations, one can simplify the general formulation within the asymptotic long-wave limit to a fourth-order partial differential equation for the film thickness h ; an equivalent formulation can be obtained by minimizing an appropriate free energy, commonly carried out within the framework of gradient flow modeling, see, for example the study by Thiele et al. [71]. The relevant equation, given here in nondimensional form [39], is

$$\frac{\partial h}{\partial t} + \nabla \cdot (Ch^3 \tilde{\nabla} \nabla^2 h + h^3 \Pi'_s(h) \tilde{\nabla} h) = 0. \quad (1)$$

Here, the film is assumed to spread on a substrate $z = 0$ (the (x, y) -plane), and $\tilde{\nabla}$ is a modified gradient operator, which accounts for the fact that the azimuthal angle $\varphi(x, y)$ in the director field description ($\mathbf{n} = (\sin \theta \cos \varphi, \sin \theta \sin \varphi, \cos \theta)$) leads to directionally dependent spreading rates:

$$\tilde{\nabla} = \left(\lambda I + \nu \begin{bmatrix} \cos 2\varphi & \sin 2\varphi \\ \sin 2\varphi & -\cos 2\varphi \end{bmatrix} \right) \quad (2)$$

where $\lambda > \nu > 0$ are dimensionless viscosities. The dimensionless number C is an inverse capillary number representing the ratio of surface tension to viscous forces, and the key term $\Pi_s(h)$ is a ‘structural disjoining pressure’, accounting for both the fluid/solid interaction potential, as well as elastic effects (including weak free surface anchoring and strong planar substrate anchoring). One

choice that appears to be appropriate (see Ref. [39**] for further discussion) is

$$\Pi_s(h) = \mathcal{K} \left[\left(\frac{b}{h} \right)^{n_1} - \left(\frac{b}{h} \right)^{n_2} \right] + \frac{\mathcal{N}}{2} \theta_s^2, \quad (3)$$

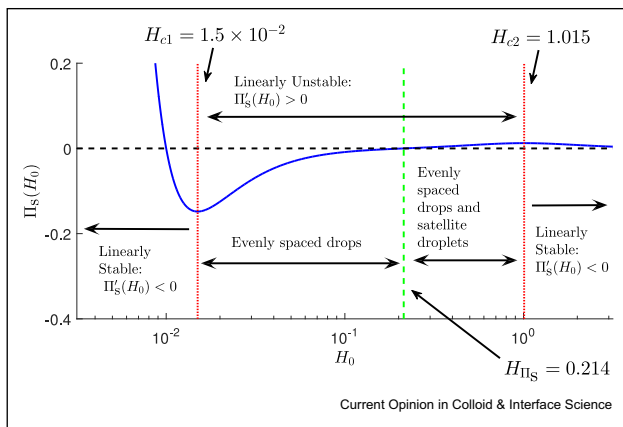
the first two terms being a widely used form of the usual disjoining pressure (with, e.g. $(n_1, n_2) = (3, 2)$), with \mathcal{K} proportional to the Hamaker constant. The parameter $b > 0$ appearing here is a dimensionless equilibrium (precursor) film thickness: the film height in (1) will always be strictly positive, with $h \geq b$, and the problem of the moving contact line singularity is avoided. The typical form of $\Pi_s(h)$ is shown in Figure 2 for $(n_1, n_2) = (3, 2)$. We note that the unstable range of film thicknesses shown also in Figure 2 may be related to the range of ‘forbidden thicknesses’, whose existence is supported by physical experiments [9].

The term proportional to \mathcal{N} (an inverse Ericksen number representing the ratio of elastic to viscous forces in the bulk NLC) models the elastic contributions within the layer [36, 45] (We note here that in some of the early work on such systems, e.g. Ref. [5], a missing term in the stress balance led to a different sign for this term; this was corrected in later work [43, 45].) Briefly, strong planar substrate anchoring at $z = 0$ is assumed, with $\varphi(x, y)$ specified there, as well as weak homeotropic anchoring at the free surface $z = h$. The director polar angle θ in \mathbf{n} takes the form

$$\theta = \frac{\pi}{2} (1 - \frac{z}{h} m(h)),$$

where the function $m(h)$ is a relaxation function that relates directly to the free surface anchoring energy [44] and can be chosen to correspond to any desired surface energy

Figure 2



Structural disjoining pressure as a function of film height (in units of 100 nm) for a typical NLC film. Various regimes shown are discussed in the text, from Ref. [39].

model (e.g. Rapini-Papoular [62]). For the purpose of maintaining a simple closed-form model, one can choose [39**, 45].

$$m(h) = g(h) \frac{h^2}{h^2 + \beta^2}, \quad g(h) = \frac{1}{2} \left[1 + \tanh \left(\frac{h - 2b}{w} \right) \right], \quad (4)$$

in which β is the thickness scale at which the bulk elastic energy is comparable with the free surface anchoring energy, and $g(h)$ is a ‘cutoff’ function (controlled by w) that forces the free surface anchoring direction to relax to that of the substrate when the film thickness is close to the equilibrium value, b (discussed in more detail later in the text).

Note that with this form of the director field, thicker NLC films are in the hybrid aligned nematic state, whereas films close to the equilibrium thickness have a director field nearly homogeneous across the film height. This transition between the states is in agreement with several other models, for example Refs. [9, 14, 49, 48, 78]. Furthermore, the lengthscale β may be related to the extrapolation length discussed in the literature [14, 20, 79].

The constant \mathcal{K} in (3) is related to the (apparent) contact angle α via the spreading parameter S , which in turn is related to the stored energy per unit area of the film [18]:

$$S = 1 - \cos \alpha = - \int_b^\infty \Pi_s(h) dh. \quad (5)$$

Substituting for Π_s from (3) and rearranging, we find (assuming small α , consistent with the thin film assumption, and retaining only leading-order terms)

$$\frac{1}{b} \left(\frac{\alpha}{H_0} \right)^2 \mathcal{C} \approx \mathcal{K} - \frac{\mathcal{N}}{\pi b \beta}, \quad (6)$$

where H_0 is the (appropriately scaled) film thickness. If $\mathcal{N} = 0$ or $\beta \rightarrow \infty$, we have the usual Newtonian balance between surface tension and disjoining forces [18]. The term in \mathcal{N} represents the effect of the free surface anchoring (hence vanishes in the weak anchoring limit, $\beta \rightarrow \infty$). Equation (6) predicts that, with sufficiently strong anchoring (sufficiently small β), the nematic nature of the fluid can significantly affect spreading and could determine whether partial or total wetting occurs (a nonpositive value of the right-hand side indicates total wetting). Note that Eq. (6) is specific to the case of strong planar substrate anchoring and weak homeotropic free surface anchoring: different conditions will lead to different contact angle

laws. Before closing this section, we digress slightly from the modeling specifics of the problem to point out that the question of the appropriate form of disjoining pressure $\Pi_s(h)$ in the context of NLC films is a long-standing one which, together with the previously mentioned issue of resolving the molecular structure of the NLC film (particularly under dewetting), has received attention from several authors. Figure 3(a) (from Ref. [58]) shows an example of the suggested orientation of the NLC molecules, both in the bulk film and in the precursor layer. Note that the proposed form of disjoining pressure sketched in Figure 3(b) has the same qualitative features as that described in this section and shown in Figure 2. Although we discuss the relevance of the particular form of $\Pi_s(h)$ to film stability further in the following section, we note that at this point only the basic features of the form of $\Pi(h)$ can

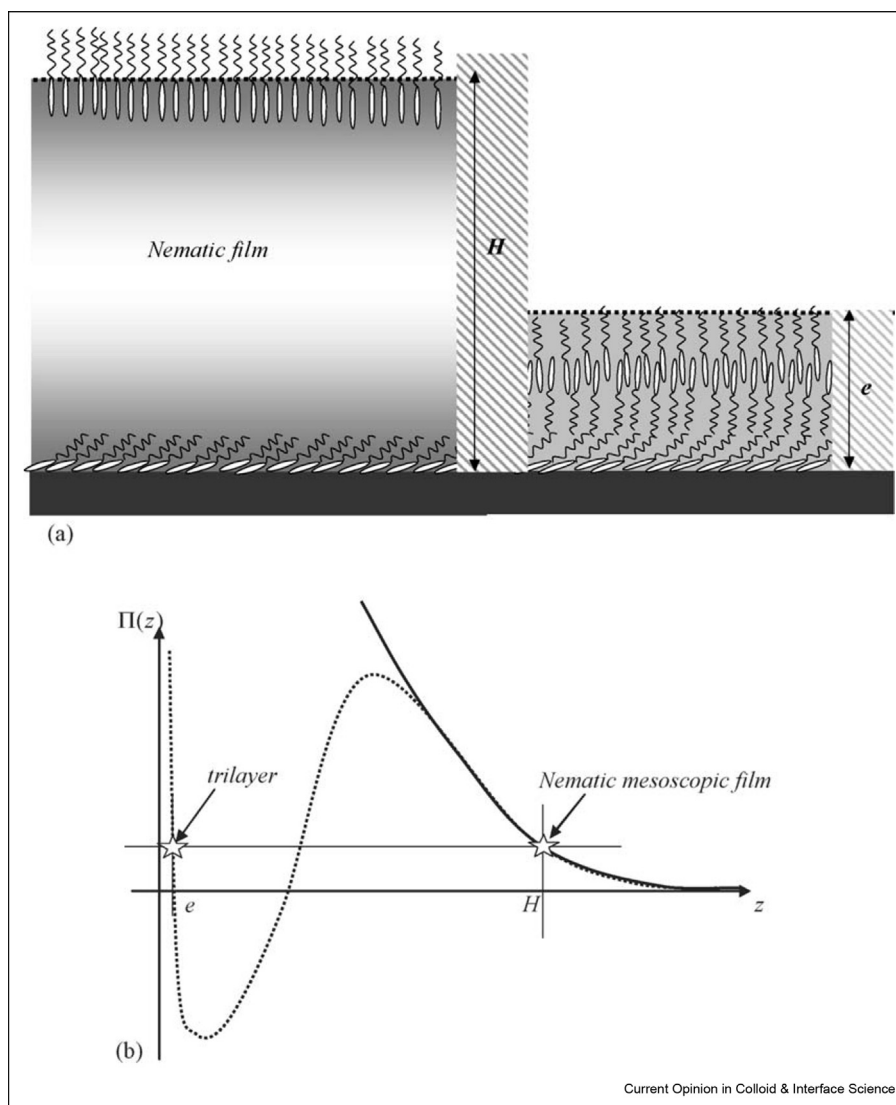
be extracted directly from the experiments. The lack of detailed understanding of the disjoining pressure and of the relevant physical mechanisms determining its functional dependence on film thickness (and possibly other quantities) seems to be the most serious limitation of the described theoretical model.

Instabilities

Two-dimensional films: disjoining pressure and satellite drops

A basic understanding of the stability properties of NLC films can be reached via linear stability analysis (LSA), which provides the following dispersion relation for growth of a sinusoidal perturbation to a flat film of thickness $h = H_0$ [39]

Figure 3



(a) Proposed orientation of NLC molecules for a mesoscopic film (left) and within the precursor, where a 'trilayer' is assumed to form on the scale of the equilibrium film thickness, see Figure 2. (b) Suggested form of disjoining pressure (note that the equilibrium film thickness is denoted by 'e' in this figure in contrast to 'b' used elsewhere in the text), from Ref. [58*].

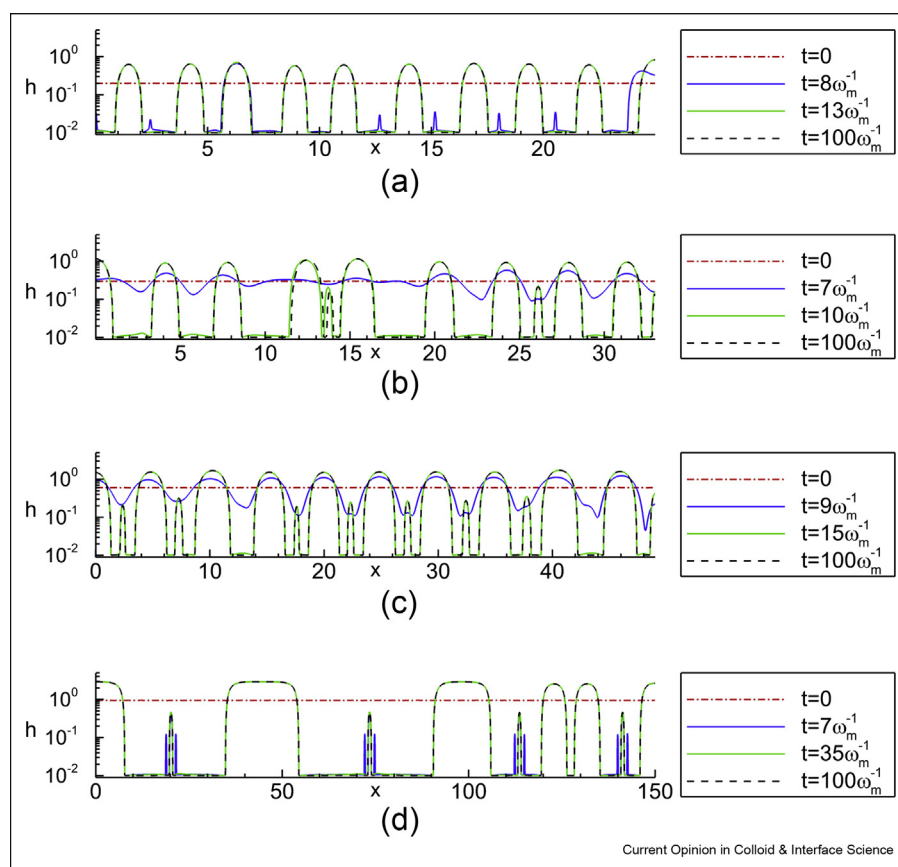
$$\omega = -H_0^3[\mathcal{C}q^2 - \Pi'_s(H_0)]q^2, \quad (7)$$

where ω is the growth rate, and q is the wave number. The conclusion is that the film is always unstable where $\Pi'_s(H_0) > 0$. Figure 2 shows a plot of $\Pi_s(H_0)$ for parameters corresponding to physical experiments [20]. The figure indicates that a range of unstable film heights is expected (between the red dotted lines), separating regions of thin and thick stable film heights, consistent with the experiments [20,30]. It should, however, be noted that quantitative comparison with experimental results is nontrivial because the parameters entering the above-mentioned dispersion relation are not precisely known; see the study by Lam et al. [39**] for detailed discussion regarding the comparison between LSA results and experiments.

Although LSA should indicate when a flat film is unstable, and may provide some insight regarding the wavelength of patterns that emerge, simulations of nonlinear evolution governed by Eq. (1) suggest that the system can exhibit a wide range of intriguing behaviors. Figure 4 shows an example of simulation results for two-dimensional films of varied thickness. First, we note that

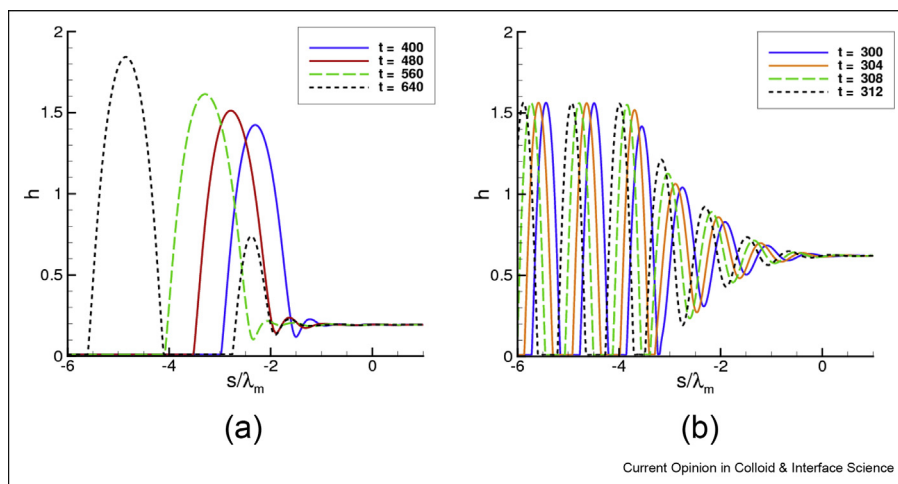
simulations of a film perturbed by a random superposition of small-amplitude sinusoidal modes are well predicted by LSA [39**]. Numerically, it is found that if the film height H_0 is in the unstable regime and $\Pi_s(H_0) < 0$, the LSA predictions hold well into the nonlinear regime, with droplets of uniform spacing, close to $2\pi/q_m$ (q_m the fastest-growing wavenumber), persisting for all times simulated. For $\Pi_s(H_0) > 0$, however, in addition to uniformly spaced droplets, one finds interspersed smaller ‘satellite’ droplets, not predicted by the LSA, providing strong numerical evidence that positive values for the disjoining pressure lead to formation of satellite drops. In the present context, such positive values are due to the nematic nature of the film and the inclusion of the elastic energy associated with the director field in the formulation: in other contexts, such values could be due to other effects, such as the presence of a complex substrate for polymer films [4, 67], or to intrinsic fluid properties in the case of ferrofluids [69]. It will be of interest to verify the generality of this finding because satellite drops are relevant in a variety of applications, in particular related to printing.

Figure 4



Free surface evolution for various initial average film thicknesses, H_0 . Note the persistent satellite droplets for thicker films. Films of base thickness larger than $H_0 = 1$ (corresponding to 100 nm) are linearly stable. Here, ω_m is the (dimensionless) growth rate of the most unstable mode, λ_m , and the domain size is $10\lambda_m$. The initial condition is a flat film perturbed by harmonic perturbations of infinitesimal random amplitudes, from Ref. [39**].

Figure 5



Typical evolution of the film thickness in the reference frame $s = x - v_{\text{msc}}t$ traveling with linear speed v_{msc} for two different (linearly unstable) film thicknesses, 0.2 (a) and 0.6 (b). The s -axis is scaled by λ_m to highlight departure from the LSA predictions in (b). The times given in the legends can be related to the LSA time scale, $1/\omega_m$, with ω_m given in Figure 4, from Ref. [39**].

Analysis based on marginal stability criteria

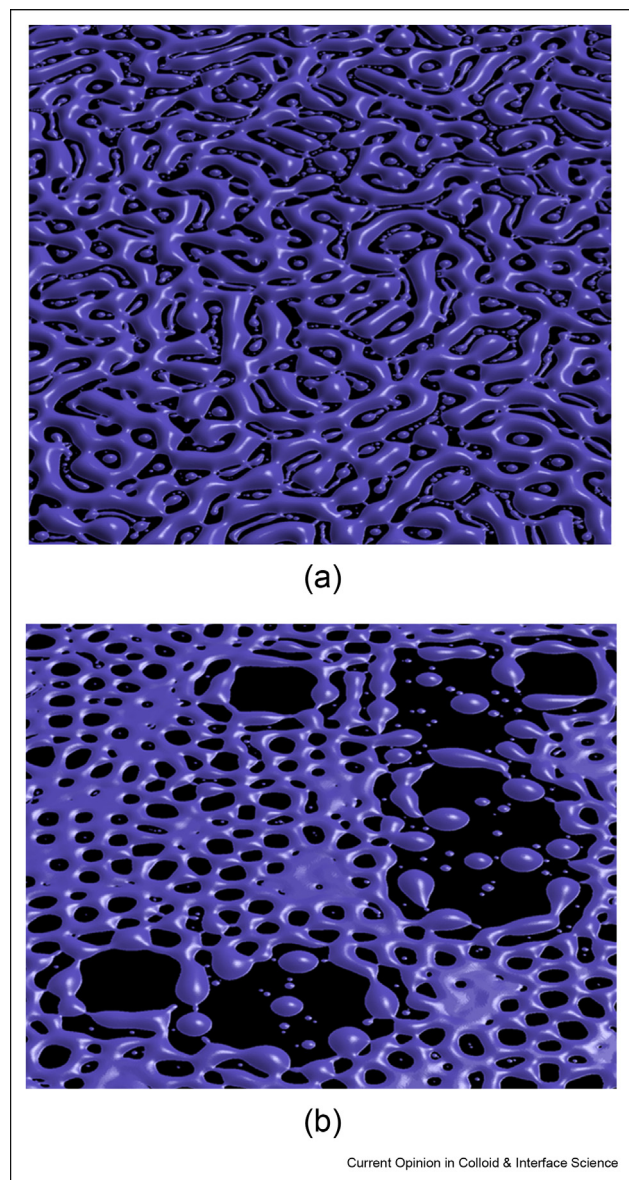
More complex dynamics are observed when a localized perturbation is applied to a flat film. In the linearly unstable regime, the initial perturbation is seen to lead first to a dewetted patch (nucleation), which increases in size. Depending on the film thickness (other parameters being fixed), the initial dewetted patch may remain isolated for a long time, or its presence may trigger a complicated cascade of dewetting events, with attendant drop formation. The wavelength of the pattern formed (droplet spacing) may differ significantly from the LSA predictions. The drop spacing and the film breakup time are not yet well understood, particularly for films whose thickness H_0 is close to the zero of the structural disjoining pressure $\Pi_s(H_0)$, see (Figure 2). The evolution of the instability suggests that the problem may involve front propagation into a possibly unstable state. This topic has been considered in a number of different systems and poses interesting mathematical challenges, with some progress reached using marginal stability criteria (MSCs), discussed further in the following. The standard example, which is well understood, is that of a nonlinear diffusion equation $\partial_t u = \partial_{xx} u + f(u)$, in particular the Fisher–Kolmogorov equation, where $f(u) = u - u^3$ [11,13,33,76]. Although strong results exist for front propagation away from a localized perturbation, an extension to more complicated systems is not trivial. Although there is no proof that MSC concepts are strictly valid, they are known to apply to a wide range of systems, including crystal growth [41], instabilities of cylindrical membranes [2,3], liquid drops in extensional flow [59, 60], and have been also recently considered in the context of thin films [35,70]. We also note the connection to the study

of bifurcation analysis in the context of the Cahn–Hilliard equation [26].

The details of MSCs are beyond the scope of the presentation here, and we give just an outline (excellent review articles are available that provide significant discussion and background [11,76], including consideration of MSCs in the context of the Kuramoto–Sivashinsky and Cahn–Hilliard equations). A key idea is this: if we know how fast the front propagates into a (possibly) unstable state, we should be able to correlate the speed of propagation with the wavenumber at which instability develops. Regarding the speed of propagation, the primary MSC result is that, under certain conditions, the speed selected is that at which the stability properties of the system change, that is, the system is in a marginally stable state. One approach is to approximate the front shape by the form $\exp(ik^*x + \omega(k^*)t)$, where k^* is the point of the stationary phase ($\omega, k^* \in \mathbb{C}$). Then, the linear MSC states that the system chooses the front velocity, v_{msc} , for which the exponential neither grows nor decays [13]. An alternative approach [6, 11] states that if a front in the moving reference frame $u(x - vt)$ is perturbed slightly, it is stable if it outruns the perturbation and unstable otherwise. In either case, the stable front with the lowest velocity is selected. Nonlinear effects may lead to modification (an increase) of the propagation velocity [76]; however, for many systems, the linear results are applicable [11, 54, 60].

The linear MSC requires that the front itself is not significantly perturbed by the breakup process, which appears to be the case for the considered system. One idea is to focus on the region close to the front itself and

Figure 6



Computational results for initially infinitesimal perturbations of global character (a) and a combination of infinitesimal and strong localized perturbations (b), from Ref. [38].

represent it as a superposition of Fourier modes as discussed previously. The linear MSC then predicts

$$v_{\text{msc}} = \frac{\Re(\omega^*)}{\Im(k^*)}; \Re\left(\frac{\partial\omega}{\partial k}\right)\Big|_{k^*} = 0; v_{\text{msc}} = -\Im\left(\frac{\partial\omega}{\partial k}\right)\Big|_{k^*}, \quad (8)$$

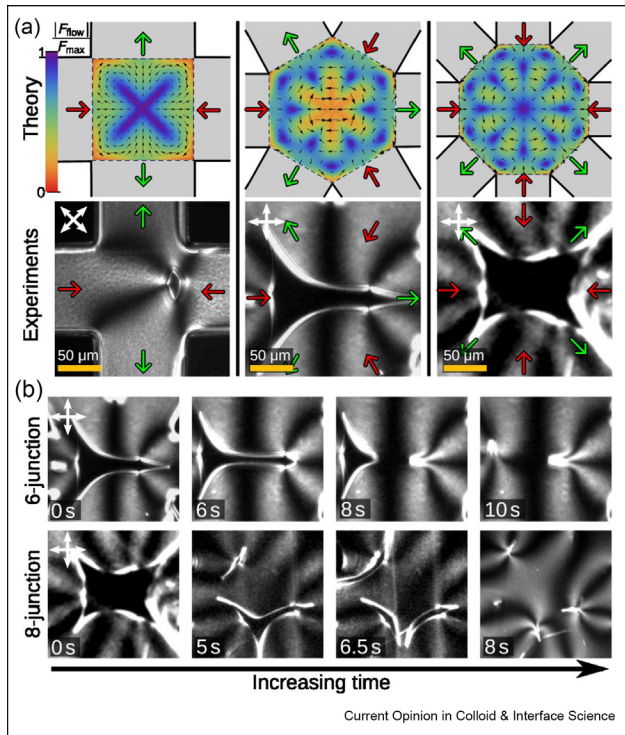
where $\omega^* = \omega(k^*)$. These relations can be used to fix k^* and v_{msc} , by obtaining the values of ω from the simulations. Further discussion regarding how to connect in practical terms the outlined theory and the results of

simulations can be found in the study by Lam et al. [39**]. Here, we limit ourselves to one example illustrating how the unperturbed thickness of (linearly unstable) films could play a crucial role in determining their evolution. Figure 5 shows two film thicknesses initially perturbed by a localized perturbation (one could think of such a perturbation as modeling a defect in the substrate or in the film itself or the presence of some external disturbance such as a speck of dust). For the parameters considered, see the study by Lam et al. [39**] for full details; for thinner films, the distance between emerging droplets may be significantly larger than the dominant wavelength λ_m predicted by the LSA (as is the case in Figure 5a), whereas for a thicker film (Figure 5b), the distance between the drops corresponds closely to λ_m . These findings suggest a possible explanation for the difference between the spinodal and nucleation types of instability discussed extensively in the context of other fluids [4, 67, 72]. We note, however, that there is still no clear answer to a rather straightforward question: what is the average distance between the drops that form in the nucleation regime, such as in Figure 5a? This is one of the open questions of relevance not only to NLCs but also to other Newtonian and complex fluids.

Computational results in three spatial dimensions

Computing the nonlinear evolution of NLCs on large domains in three dimensions (3D) (3D in the physical sense; two dimensions in the mathematical sense because the film thickness is a function of two in-plane spatial variables, $h(x, y, t)$, within the long-wave model) is a computationally demanding endeavor, much more so than the mathematically similar formulation resulting from, for example, Cahn–Hilliard spinodal decomposition. The reason for this is the need to fully resolve short length scales, which are typically specified by the range of substrate–film interaction forces and therefore by the equilibrium film thickness. Although the exact range of these forces is not always clear in any particular experimental setup, in general, it is expected to be on the nanoscale range or even smaller [38*]. Resolving such small scales (even for films of thickness on the scale of 100 or so nanometers) leads to large discretized systems of equations. Recalling, furthermore, that the size of the time step may be limited not only by accuracy but also by stability criteria makes it clear why significant care is required in carrying out simulations on large computing domains. Although a significant body of work focusing on the development of computational methods has been established through the last couple of decades, this is still a very active field of research, with new methods and computing software being developed. Regarding relatively recent developments in this direction, it is worth mentioning open source repositories such as OOMPH library [28,29] and the GPU-based software GADIT [37, 38*], with the latter used to produce computational results in the context of NLC films, discussed next.

Figure 7



Examples of defects at flow junctions. **(a)** (upper): the fluid force field for different defect types (lower): images of defects right after formation; **(b)**: defect decay over time for defects of winding number 2 (upper) and 3 (lower), from Ref. [25].

Based on the discussion in Sections Two-dimensional films: disjoining pressure and satellite drops and Analysis based on marginal stability criteria, it is clear that

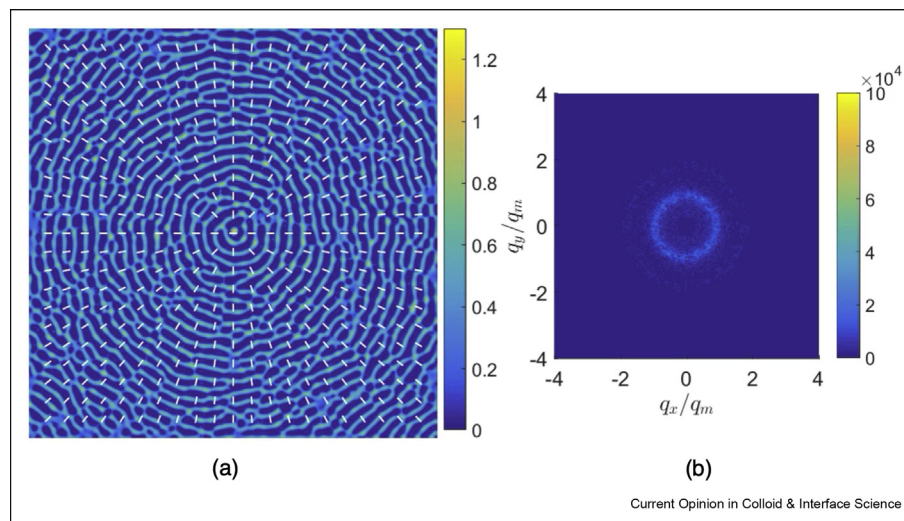
rather complex temporal evolution and pattern formation can be expected. In the 3D, it is more difficult to discuss in precise terms the details of instability development because of the larger parameter space, so we focus here on one particular question, namely, what is the influence of the type of perturbation initially imposed on the resulting film dynamics (We note that the time evolution in the simulations discussed here is fully deterministic; to understand the influence of stochasticity, one needs to consider a stochastic variant of the evolution Eq. (1), a topic analyzed recently in the context of Newtonian films [17, 52].)

Figure 6 shows the results of two simulations, which differ only in the initial condition: in (a), only infinitesimal (global) perturbations are included, whereas in (b), both global and (finite-size) local perturbations are imposed. The idea here is that such simulations could model film evolution in the presence of small-scale surface perturbations (a) or in the presence of strong but localized perturbations (nucleation centers; (b)). The presence of such large perturbations and their influence can be also seen in the experiments, see Figure 1. In the context of NLC films, such nucleation centers could possibly be also due to the presence of defects in the director field, briefly discussed next.

Defects

The presence of defects in the director field is specific to LC films. Figure 7 shows an example of such structures in experiments (due to Giomi et al. [25]), where different defect types and their evolution are visible.

Figure 8



The example of the influence of an isolated defect in the director field on the instability of a film perturbed initially by random noise. **(a)** Film profile, with spatially varying substrate anchoring (overlaid in white). **(b)** Fourier spectrum of the pattern, where q_m is the most unstable wavenumber, and q_x and q_y are the wavenumbers in the x and y directions, respectively.

Modeling the presence of defects is nontrivial because these structures involve ‘singularities’—significant changes of the director field over short scales. Therefore, at the defect location, the underlying Leslie-Ericksen model breaks down (an accurate description of defects in NLCs requires a more sophisticated model, such as Landau-De Gennes [12], with an order parameter that allows for localized ‘melting’ of the director structure at the defect core); nonetheless, we expect that the model discussed so far may provide a reasonable qualitative indication of how the presence of a defect influences the overlying flow, in particular, the film thickness evolution. Here, we limit ourselves to a brief outline of recent progress in describing the evolution of NLC films in the presence of defects, with the caveat that this direction of research is still ongoing.

The simplest way to introduce defects within the formulation discussed so far is via specifying the function $\varphi(x, y)$ that determines the preferred director orientation at the substrate. The effect of azimuthal director orientation on the film stability is a subject of ongoing research, for example Ref. [40], and here, we show just one example, see Figure 8, illustrating the effect of a $s = +1$ defect (s being the topological winding number of the defect) on the film stability. We observe that the azimuthal orientation of the director field influences strongly film instability and dewetting.

Conclusions

Thin NLC films are fascinating systems that bridge the divide between Newtonian and complex fluids. Many aspects of the modeling are furthermore of relevance to the emerging field of modeling active matter; some notable examples include modeling cell motility [46, 47, 73] and active gels [34]. In this review, we have covered only one rather narrow aspect of an otherwise very rich system; even so, however, this focused discussion reveals many questions whose answers are only just beginning to be formulated. These questions include the role of the nematic nature of the film on instability development, the connection between NLC films and other Newtonian and non-Newtonian films, and the role of ‘defects’, which may be present in the director field, in instability development. We hope that this brief review will inspire new research, both theoretical and experimental, which will in turn lead to a better understanding of the many unresolved issues involved in the dynamics of thin nematic LC films on the nanoscale.

Declaration of competing interest

The authors declare that they have no known competing financial interests or personal relationships that could have appeared to influence the work reported in this article.

References

Papers of particular interest, published within the period of review, have been highlighted as:

* of special interest

** of outstanding interest

- Allen M: **Molecular simulation of liquid crystals**. *Mol Phys* 2019, **117**:2391–2417.
- Bar-Ziv R, Moses E: **Instability and “pearling” states produced in tubular membranes by competition of curvature and tension**. *Phys Rev Lett* 1994, **73**:1392.
- Bar-Ziv R, Tlusty T, Moses E: **Critical dynamics in pearling instability of membranes**. *Phys Rev Lett* 1997, **79**:1158.
- Becker J, Grün G, Seemann R, Mantz H, Jacobs K, Mecke KR, Blossey R: **Complex dewetting scenarios captured by thin-film models**. *Nature Mat* 2003, **2**:59.
- Ben Amar M, Cummings LJ: **Fingering instabilities in driven thin nematic films**. *Phys Fluids* 2001, **13**:1160.
- Ben-Jacob E, Brand H, Dee G, Kramer L, Langer JS: **Pattern formation in nonlinear dissipative systems**. *Physica D* 1985, **14**:348.
- Bonn D, Eggers J, Indekeu J, Meunier J, Rolley E: **Wetting and spreading**. *Rev Mod Phys* 2009, **81**:739.
- Carou J, Mottram N, Wilson S, Duffy B: **A mathematical model for blade coating of a nematic liquid crystal**. *Liq Cryst* 2007, **35**:621.
- Cazabat AM, Delabre U, Richard C, Sang YYC: **Experimental study of hybrid nematic wetting films**. *Adv Colloid Interface Sci* 2011, **168**:29.
- Craster R, Matar O: **Dynamics and stability of thin liquid films**. *Rev Mod Phys* 2009, **81**:1131.
- Cross MC, Hohenberg PC: **Pattern formation outside of equilibrium**. *Rev Mod Phys* 1993, **65**:851.
- De Gennes PG, Prost J: **The physics of liquid crystals**. In *International series of monographs on physics*. 2 ed. Oxford University Press; 1995.
- Dee G, Langer JS: **Propagating pattern selection**. *Phys Rev Lett* 1983, **50**:383.
- Delabre U, Richard C, Cazabat AM: **Thin nematic films on liquid substrates**. *J Phys Chem B* 2009, **113**:3647.
- Delabre U, Richard C, Guéna G, Meunier J, Cazabat AM: **Nematic pancakes revisited**. *Langmuir* 2008, **24**:3998.
- Demeter G, Krimer DO: **Light-induced dynamics in nematic liquid crystals: a fascinating world of complex nonlinear phenomena**. *Phys Rep* 2007, **448**:133.
- Nonequilibrium physics: From complex fluids to biological systems II. Systems with nematic order.
- Diez JA, González AG, Fernández R: **Metallic-thin-film instability with spatially correlated thermal noise**. *Phys Rev E* 2016, **93**, 013120.
- Diez JA, Kondic L: **On the breakup of fluid films of finite and infinite extent**. *Phys Fluids* 2007, **19**, 072107.
- Edwards A, Brown C, Newton M, McHale G: **Dielectrowetting: the past, present and future**. *Curr Opin Colloid Interface Sci* 2018, **36**:28–36.
- A timely and comprehensive review of how electric field gradients may be harnessed to guide spreading and dewetting of dielectric fluids on a substrate, and the many potential applications of such dielectrowetting.
- van Effenterre D, Ober R, Valignat MP, Cazabat AM: **Binary separation in very thin nematic films: thickness and phase coexistence**. *Phys Rev Lett* 2001, **87**:125701.
- van Effenterre D, Valignat MP: **Stability of thin nematic films**. *Eur. Phys. J. E* 2003, **12**:367.
- Ericksen J: **Anisotropic fluids**. *Arch Ration Mech Anal* 1960, **4**: 231.

23. Gartland EC: **Electric-field-induced instabilities in nematic liquid crystals**. *SIAM J Appl Math* 2021, **81**:304–334.
24. Gay JG, Berne BJ: **Modification of the overlap potential to mimic a linear site potential**. *J Chem Phys* 1981, **74**: 3316–3319.
25. Giomi L, Kos Ž, Ravnik M, Sengupta A: **Cross-talk between topological defects in different fields revealed by nematic microfluidics**. *Proc Natl Acad Sci Unit States Am* 2017: 5771–5777.
26. Goh R, Scheel A: **Hopf bifurcation from fronts in the Cahn-Hilliard equation**. *Arch Ration Mech Anal* 2015, **217**:1219.
27. Harth K, Stannarius R: **Deep holes in free-standing smectic c films**. *Ferroelectrics* 2014, **468**:92–100.
28. Hazel A, Heil M: *OOMPOLIB*. 2019.
- This library is of importance to researchers working on numerical solutions of nonlinear partial differential equations governing thin film flows, particularly those with flow–structure interaction. <http://oomph-lib.maths.man.ac.uk/doc/html/index.html>.
29. Heil M, Hazel AL: **Oomph-lib - an object-oriented multi-physics finite-element library**. In *Fluid-structure interaction: modelling, simulation, optimisation*. Edited by Bungartz HJ, Schäfer M, Springer; 2006:19.
30. Herminghaus S, Jacobs K, Mecke K, Bischof J, Fery A, Ibn-Elhaj M, Schlagowski S: **Spinodal dewetting in liquid crystal and liquid metal films**. *Science* 1998, **282**:916.
- One of the first experimental studies discussing dewetting instabilities of nematic liquid crystal films on nanoscale.
31. Jákli A, Lavrentovich OD, Selinger JV: **Physics of liquid crystals of bent-shaped molecules**. *Rev Mod Phys* 2018, **90**, 045004.
- This paper reviews experimental and theoretical results that highlight the important implications of a “bent core” molecular shape for macroscopic physical manifestations of Liquid Crystal behavior.
32. Jerome R: **Surface effects and anchoring in liquid crystals**. *Rep Prog Phys* 1991, **54**:391.
33. Kessler DA, Ner Z, Sander LM: **Front propagation: precursors, cutoffs, and structural stability**. *Phys Rev E* 1998, **58**:107.
34. Kitavtsev G, Münch A, Wagner B: **Thin-film models for an active gel**. *Proc. R. Soc. A* 2018, **474**:20170828.
35. Köpf MH, Gurevich SV, Friedrich R, Thiele U: **Substrate-mediated pattern formation in monolayer transfer: a reduced model**. *New J Phys* 2012, **14**, 023016.
36. Lam MA, Cummings LJ, Lin TS, Kondic L: **Three-dimensional coating flow of nematic liquid crystal on an inclined substrate**. *Eur J Appl Math* 2015, **25**:647.
37. Lam MAYH: *GADIT: thin film GPU code at GitHub repository*. 2019. <https://github.com/mayhl/>.
38. Lam MAYH, Cummings LJ, Kondic L: **Computing dynamics of thin films via large scale GPU-based simulations**. *J Comput Phys X* 2018a, **2**:100001.
- This paper presents an algorithm and coding details of relevance to numerical solutions of the nonlinear partial differential equation governing film evolution.
39. Lam MAYH, Cummings LJ, Kondic L: **Stability of thin fluid films characterised by a complex form of effective disjoining pressure**. *J Fluid Mech* 2018b, **841**:925.
- Detailed discussion of the influence of the functional form of disjoining pressure on instability development.
40. Lam MAYH, Kondic L, Cummings LJ: **Effects of spatially-varying substrate anchoring on instabilities and dewetting of thin nematic liquid crystal films**. *Soft Matter* 2020, **16**: 10187.
41. Langer JS, Muller-Krumbhaar H: **Mode selection in a dendrite-like nonlinear system**. *Phys. Rev. A* 1982, **27**:499.
42. Leslie F: **Some constitutive equations for anisotropic fluids**. *Q J Mech Appl Math* 1966, **19**:357–370.
43. Lin TS, Cummings LJ, Archer AJ, Kondic L, Thiele U: **Note on the hydrodynamic description of thin nematic films: strong anchoring model**. *Phys Fluids* 2013a, **25**, 082102.
44. Lin TS, Kondic L, Filippov A: **Thin films flowing down inverted substrates: three dimensional flow**. *Phys Fluids* 2012, **24**, 022105.
45. Lin TS, Kondic L, Thiele U, Cummings LJ: **Modeling spreading dynamics of liquid crystals in three spatial dimensions**. *J Fluid Mech* 2013b, **729**:214.
46. Loisy A, Eggers J, Liverpool TB: **Tractionless self-propulsion of active drops**. *Phys Rev Lett* 2019, **123**:248006.
47. Loisy A, Eggers J, Liverpool TB: **How many ways a cell can move: the modes of self-propulsion of an active drop**. *Soft Matter* 2020, **16**:3106–3124.
48. Manyuhina OV, Ben Amar M: **Thin nematic films: anchoring effects and stripe instability revisited**. *Phys Lett A* 2013, **377**: 1003.
49. Manyuhina OV, Cazabat AM, Ben Amar M: **Instability patterns in ultrathin nematic films: comparison between theory and experiment**. *Europhys Lett* 2010, **92**:16005.
50. Marchetti MC, Joanny JF, Ramaswamy S, Liverpool TB, Prost J, Rao M, Simha RA: **Hydrodynamics of soft active matter**. *Rev Mod Phys* 2013, **85**:1143–1189.
51. McHale G, Brown CV, Newton MI, Wells GG, Sampara N: **Developing interface localized liquid dielectrophoresis for optical applications**. In *Optical design and testing V*. Edited by Wang Y, Du C, Hua H, Tatsuno K, Urbach HP, SPIE: International Society for Optics and Photonics; 2012:13–20.
52. Nesic S, Cuerno R, Moro E, Kondic L: **Dynamics of thin fluid films controlled by thermal fluctuations**. *Phys Rev E* 2015, **92**, 061002(R).
53. Nguyen TD, Fuentes-Cabrera M, Fowlkes JD, Rack P: **Coexistence of spinodal instability and thermal nucleation in thin-film rupture: insights from molecular levels**. *Phys Rev E* 2014, **89**, 032403.
54. Nishiura Y: *Far-from-equilibrium dynamics*. Providence: American Mathematical Society; 1999.
55. Palffy-Muhoray P: **The diverse world of liquid crystals**. *Phys Today* 2014, **60**:54.
56. Poulard C, Cazabat AM: **Spontaneous spreading of nematic liquid crystals**. *Langmuir* 2005a, **21**:6270.
57. Poulard C, Cazabat AM: **Spontaneous spreading of nematic liquid crystals**. *Langmuir* 2005b, **21**:6270.
58. Poulard C, Voué M, De Coninck J, Cazabat AM: **Spreading of nematic liquid crystals on hydrophobic substrates**. *Colloid Surface Physicochem Eng Aspect* 2006, **282**:240.
- Discussion of the functional form of disjoining pressure in the context of stability of nematic liquid crystal films.
59. Powers TR, Goldstein RE: **Pearling and Pinching: propagation of Rayleigh instabilities**. *Phys Rev Lett* 1997, **78**:2555.
60. Powers TR, Zhang D, Goldstein RE, Stone HA: **Propagation of a topological transition: the Rayleigh instability**. *Phys Fluids* 1998, **10**:1052.
61. Quintans Carou J, Duffy BR, Mottram NJ, Wilson SK: **Shear-driven and pressure-driven flow of a nematic liquid crystal in a slowly varying channel**. *Phys Fluids* 2006, **18**, 027105.
62. Rapini A, Papoular M: **Distorsion d'une lamelle nématique sous champ magnétique conditions d'ancrage aux parois**. *J Phys Colloq* 1969, **30**:C4–C54.
63. Rey AD: **Liquid crystal models of biological materials and processes**. *Soft Matter* 2010, **6**:3402–3429.
64. Rey AD, Denn MM: **Dynamical phenomena in liquid-crystalline materials**. *Annu Rev Fluid Mech* 2002, **34**:233.
65. Saintillan D: **Rheology of active fluids**. *Annu Rev Fluid Mech* 2018, **50**:563–592.

A detailed and thorough review of how the microscale details of active suspensions influence macroscale rheology, covering experimental, theoretical and computational modeling aspects.

66. Schlagowski S, Jacobs K, Herminghaus S: **Nucleation-induced undulative instability in thin films of nCB liquid crystals.** *Europhys Lett* 2002, **57**:519.
67. Seemann R, Herminghaus S, Jacobs K: **Dewetting patterns and molecular forces: a reconciliation.** *Phys Rev Lett* 2001, **86**.
68. Sengupta A: **Topological microfluidics: present and prospects.** *Liq Cryst Today* 2015, **24**:70–80.
69. Seric I, Afkhami S, Kondic L: **Interfacial instability of thin ferrofluid films under a magnetic field.** *J. Fluid Mech. Rapids* 2014, **755**:R1.
70. Tewes W, Wilczek M, Gurevich SV, Thiele U: **Self-organized dip-coating patterns of simple, partially wetting, nonvolatile liquids.** *Phys. Rev. Fluids* 2019, **4**:123903.
71. Thiele U, Archer A, Pismen L: **Gradient dynamics models for liquid films with soluble surfactant.** *Phys. Rev. Fluids* 2016, **1**, 083903.
72. Thiele U, Velarde MG, Neuffer K: **Dewetting: film rupture by nucleation in the spinodal regime.** *Phys Rev Lett* 2001, **87**, 016104.
73. Trinschek S, Stegemerten F, John K, Thiele U: **Thin-film modeling of resting and moving active droplets.** *Phys Rev E* 2020, **101**, 062802.
74. van Effenterre D, Valignat MP: **Stability of thin nematic films.** *Eur. Phys. J. E* 2003, **12**:367.
75. van Effenterre D, Valignat MP, Roux D: **Coupling between the nematic/isotropic transition and a thickness transition: a theoretical approach.** *Europhys Lett* 2003, **62**: 526–532.
76. van Saarloos W: **Front propagation into unstable states.** *Phys Rep* 2003, **386**:29.
77. Vandenbrouck F, Valignat MP, Cazabat AM: **Thin nematic films: metastability and spinodal dewetting.** *Phys Rev Lett* 1999, **82**: 2693.
78. Zihlerl P, Podgornik R, Zumer S: **Pseudo-casimir structural force drives spinodal dewetting in nematic liquid crystals.** *Phys Rev Lett* 2000, **84**:1228.
79. Zihlerl P, Zumer S: **Morphology and structure of thin liquid-crystalline films at nematic isotropic transition.** *Eur. Phys. J. E* 2003a, **12**:361.
80. Zihlerl P, Zumer S: **P. Zihlerl and S. Zumer respond.** *Eur. Phys. J. E* 2003b, **12**:373.